

**VASCULAR BIOLOGY, ATHEROSCLEROSIS, AND ENDOTHELIUM BIOLOGY**

PGC-1 α Regulates Normal and Pathological Angiogenesis in the Retina

Magali Saint-Geniez,^{*} Aihua Jiang,[†] Stephanie Abend,^{*} Laura Liu,[†] Harry Sweigard,[‡] Kip M. Connor,[‡] and Zoltan Arany[†]

From the Schepens Eye Research Institute,^{*} Department of Ophthalmology,[†] Massachusetts Eye and Ear Infirmary, Harvard Medical School, Boston; and The Cardiovascular Institute,[‡] Beth Israel Deaconess Medical Center, Boston

Accepted for publication
September 4, 2012.

Address correspondence to
Zoltan Arany, M.D., Ph.D.,
ECLS906, Beth Israel
Deaconess Medical Center, 330
Brookline Ave, Boston,
MA 02215. E-mail: zarany@bidmc.harvard.edu.

Neovascular diseases of the eye are the most common causes of blindness worldwide. The mechanisms underlying pathological neovascularization in the retina remain incompletely understood. PGC-1 α is a transcriptional coactivator that plays a central role in the regulation of cellular metabolism. In skeletal muscle, PGC-1 α induces VEGFA expression and powerfully promotes angiogenesis, suggesting a similar role in other tissues. This study investigates the role of PGC-1 α during normal and pathological vascularization in the retina. We show that PGC-1 α induces the expression of VEGFA in numerous retinal cells, and that PGC-1 α expression is strongly induced during postnatal retinal development, coincident with VEGFA expression and angiogenesis. PGC-1 α ^{-/-} mice have a significant reduction of early retinal vascular outgrowth, and reduced density of capillaries and number of main arteries and veins as adults. In the oxygen-induced retinopathy model of retinopathy of prematurity, PGC-1 α expression is dramatically induced in the inner nuclear layer of the retina, suggesting that PGC-1 α drives pathological neovascularization. In support of this, PGC-1 α ^{-/-} mice subjected to oxygen-induced retinopathy had decreased expression of VEGFA and were protected against pathological neovascularization. These results demonstrate that PGC-1 α regulates VEGFA in the retina and is required for normal vessel development and for pathological neovascularization. The data highlight PGC-1 α as a novel target in the treatment of neovascular diseases of the eye. (*Am J Pathol* 2013, 182: 255–265; <http://dx.doi.org/10.1016/j.ajpath.2012.09.003>)

The mature retina is a highly metabolic neural tissue with the highest oxygen consumption per unit weight of any human tissue.¹ In most mammals, the adult retina is vascularized by two independent circulatory systems: the retinal vessels that supply the inner part of the retina, and the choroidal vessels that supply the deeper section of the retina.² Retinal blood vessels normally are quiescent with respect to growth.³ However, in a variety of retinal pathologies, such as proliferative diabetic retinopathy, venous occlusion, age-related macular degeneration, and retinopathy of prematurity (ROP), abnormal angiogenic growth of vessels into the retinal tissue and/or the vitreous leads to serious vision loss.

ROP, the leading cause of blindness in premature and very-low-birth-weight infants,⁴ is caused by disorganized retinal vascular growth.⁵ Vascularization of the retina in humans is normally complete and stabilized at term. By contrast, the immature vessels of preterm infants placed in hyperoxic incubators regress in the face of increased oxygen tension (vaso-obliterative phase).⁶ Once returned to normoxia, the

insufficiently perfused retina becomes ischemic, and dramatically induces vascular endothelial growth factor A (VEGFA) and abnormal vessel growth (vaso-proliferative phase). Current approaches to the treatment of ROP only reduce the incidence of blindness by 25%, and are destructive to the retina.⁷ More recent efforts with anti-VEGF therapy have yielded promising results, underscoring the importance of VEGFA in this disease.⁸ Understanding the pathophysiology of ROP, and identifying potentially targetable

Supported by the March of Dimes (Z.A.), the Harvard Catalyst | The Harvard Clinical and Translational Science Center (Z.A. and M.S.-G.), the National Heart, Lung, and Blood Institute (Z.A.), the American Heart Association (A.J.), the American Diabetes Association (Z.A.), the Ellison Foundation (Z.A.), the National Eye Institute Training Grant (H.S.) and Core Grant for Vision Research (K.M.C.), Research to Prevent Blindness unrestricted grant to Harvard Department of Ophthalmology (K.M.C.), the NIH R01EY022084 (K.M.C.), and financial contributions from Harvard University and its affiliated academic health care centers.

M.S.-G. and A.J. contributed equally to this work.

pathways that regulate retinal VEGFA and angiogenesis, is therefore of great interest.

The transcription factor hypoxia inducible factor-1 α (HIF-1 α) has long been proposed as the main force driving retinal vascularization in both normal and pathological conditions.⁹ However, this concept has recently been challenged. For example, using genetically modified mice in which the VEGFA promoter lacks the HIF-responsive element and therefore is unable to produce VEGFA in response to HIF-1 α , Vinore et al¹⁰ showed that HIF-1 α —dependent VEGFA regulation was surprisingly not required for normal retinal vascularization. We recently described in skeletal muscle a novel and HIF-independent pathway that powerfully regulates angiogenesis, involving the transcriptional coactivator PPAR γ -coactivator-1 α (PPARGC1A; alias PGC-1 α).¹¹ PGC-1 α is a powerful regulator of mitochondria and oxidative metabolism in numerous tissues (reviewed in Kelly and Scarpulla,¹² Lin et al,¹³ Handschin and Spiegelman,¹⁴ and Arany¹⁵). In addition, we recently showed that PGC-1 α also regulates an angiogenic program, including VEGFA and other angiogenic factors, in cultured muscle cells and skeletal muscle *in vivo*.¹¹ Transgenic expression of PGC-1 α in skeletal muscle dramatically increased microvascular density, and was protective in a model of skeletal muscle ischemia. PGC-1 α , a major regulator of mitochondrial function, thus also controls a novel and powerful angiogenic pathway in skeletal muscle, suggesting that it may also do so in other tissues.

Despite the fact that the retina is one of the most metabolically active and vascularized tissues in the body, little is known about the role of PGC-1 α in the eye. Only one report recently implicated PGC-1 α in the survival of photoreceptor cells to light-induced damage.¹⁶ The identification of PGC-1 α as a novel regulator of angiogenesis, and its important role in metabolism, led us to suspect that it may play a role in retinal vascular development and in ROP. We show here that PGC-1 α is expressed in the retina, that its expression rises dramatically within the developing retina, and that PGC-1 α can induce VEGFA in retinal cells. Moreover, *PGC-1 α ^{-/-}* mice have delayed retinal vasculature outgrowth and are protected from pathological neovascularization in a model of proliferative retinopathy similar to ROP.

Materials and Methods

Animals

All animal experiments were approved by the Schepens Eye Research Institutional Animal Care and Use Committee. PGC-1 α —deficient mice have been previously described.¹⁷ Oxygen-induced retinopathy (OIR) was induced by placing postnatal day (P) 7 mice in 75 \pm 2% oxygen for 5 consecutive days, as previously described.¹⁸

Cells and Reagents

The human Müller cell line, MIO-M1 (a gift from G. Astrid Limb, Institute of Ophthalmology and Moorfields Eye

Hospital, London, UK), and the murine cone cell line, 661W (a gift from Dr. Al-Ubaidi, Department of Cell Biology, University of Oklahoma Health Sciences Center) were maintained in Dulbecco's modified Eagle's medium (DMEM) (Invitrogen/Gibco, Carlsbad, CA) supplemented with 100 IU/mL penicillin, 100 μ g/mL streptomycin (all from Gibco), and 10% heat-inactivated fetal bovine serum (Atlanta Biologicals, Lawrenceville, GA). The rat ganglion cell line, RGC-5, was maintained in DMEM with 1.0 g/L glucose (Invitrogen/Gibco) with 100 IU/mL penicillin, 100 μ g/mL streptomycin (all from Gibco), and 10% heat-inactivated fetal bovine serum (Atlanta Biologicals). ARPE-19 cells (American Type Culture Collection, Manassas, VA) were maintained in DMEM/F12 medium (Lonza, Basel, Switzerland), 100 IU/mL penicillin, 100 μ g/mL streptomycin (all from Gibco), and 10% heat-inactivated fetal bovine serum (Atlanta Biologicals). RGC5 differentiation was induced by 1 μ mol/L staurosporine in DMEM (without serum or antibiotics) for 1 hour at 37°C. All cultures were maintained in a humidified atmosphere of 95% air and 5% CO₂ at 37°C. Retrovirus and adenoviruses overexpressing PGC-1 α have been described.^{19,20} For *PGC-1 α* knock-down, MIO-M1s were infected with lentivirus carrying human *PGC-1 α* short hairpin (shPGC-1 α) plasmid or green fluorescent protein (GFP) short hairpin (shGFP) plasmid (obtained from the RNAi Consortium at the Broad Institute of Harvard and MIT) and selected for puromycin resistance. PGC-1 α expression was confirmed by quantitative PCR (qPCR) of the *PGC-1 α* gene as well as its downstream target genes. PGC-1 α expression at protein level was measured by Western blotting. MIO-M1 cells were starved in DMEM with 0.5% FBS overnight and then kept in normoxia or hypoxia (complete deprivation of oxygen) for 24 hours before harvesting for qPCR or enzyme-linked immunosorbent assay for VEGFA expression levels. VEGFA enzyme-linked immunosorbent assay was performed on conditioned media using the Human VEGF Quantikine kit (R&D Systems, Minneapolis, MN) according to the manufacturer's instructions.

qPCR

Total RNA was isolated from tissue and cells using RNA-Bee solution (Iso-Tex Diagnostics, Friendswood, TX) or the TurboCapture 384 mRNA Kit (Qiagen, Valencia, CA). RNA was reverse-transcribed using iScript (Bio-Rad Laboratories, Hercules, CA) or the High Capacity cDNA Reverse Transcription Kit (Applied Biosystems, Foster City, CA). qPCR reactions were performed using the SYBR Green Master Mix and the ABI Prism 9700 Sequence Detection System (Applied Biosystems) or the CFX384 Real-Time System (Bio-Rad) according to the manufacturers' instructions. To ensure accurate gene quantification, the PCR data were normalized to the mean of multiple internal control genes (*HRPT*, *B2M*, *ACTB*, and *TBP*),²¹ and gene expression was calculated according to the $\Delta\Delta C_T$

method. The list of genes investigated by qPCR are listed in Table 1, and the respective primers used are listed in Table 2.

Laser-Capture Microdissection

Enucleated eyes from P17 animals exposed to the OIR model and from controls were flash frozen in optimal cutting temperature compound under RNase-free conditions. Sixteen-micron sections were obtained using a cryostat (Leica 3050S; Leica Microsystems, Wetzlar, Germany), mounted on polyethylene terephthalate slides (Leica Microsystems), and then stained immediately or stored at -80°C . Before laser microdissection, sections were fixed and dehydrated in 50% then 75% ethanol, and washed in nuclease-free water (Ambion, Foster City, CA). Sections were briefly stained for 20 seconds in 0.1% toluidine blue dye (Sigma-Aldrich, St. Louis, MO), rinsed in nuclease-free water and destained in 75% ethanol. The outer nuclear layer (ONL), inner nuclear layer (INL), and ganglion cell layer (GCL) were captured using a Laser Microdissection Microscope (Model AS LMD; Leica Microsystems). Total RNA was isolated using an RNeasy Micro kit (Qiagen) and quantified by Nanodrop spectrophotometry (Thermo Fisher Scientific, Waltham, MA).

Western Blot

Cell lysates were loaded onto a NuPAGE Novex 4% to 12% Bis-Tris Gel (Invitrogen), normalized for protein content. After being separated by size, proteins were transferred to an Immobilon membrane (Millipore, Billerica, MA). The membrane was blocked with 3% milk in TBST buffer for 1 hour at room temperature and incubated with an anti-PGC-1 α antibody (ST1202, 1:1000; Calbiochem/Millipore) in 3% milk in TBST buffer overnight at 4°C . The membrane was then incubated with secondary antibody (1:10,000; Jackson ImmunoResearch Laboratories, West

Grove, PA) in 3% milk in TBST buffer for 1 hour at room temperature.

Spectral-Domain Optical Coherence Tomography Imaging and ONL Thickness Quantification

Images centered on the optic nerve head were acquired on live anesthetized animals with spectral-domain optical coherence tomography (SD-OCT) (Bioptigen, Research Triangle Park, NC). Volume analysis was performed using 100 horizontal, raster, and consecutive B-scan lines, each one composed of 1200 A-scans. The volume size was 1.6×1.6 mm. ONL thickness was measured using Photoshop CS4 (Adobe Systems, San Jose, CA) on cross-sectional areas every 100 μm from the optic nerve on each side.

Histology and Immunohistochemistry

For histology, whole eyes were fixed with 10% formalin and prepared for paraffin embedding and sectioning. Sagittal sections were stained with hematoxylin and eosin. Whole retinas were dissected and immunostained as previously described.²² Briefly, whole retinas were blocked 2 hours with 1% bovine serum albumin in PBS containing 0.1 mmol/L CaCl_2 and 0.1 mmol/L MgCl_2 and incubated overnight with the appropriate antibody: Alexa 488-labeled (I21411; Invitrogen) or Alexa 594-labeled isolectin IB4 (I21413; Invitrogen), anti-smooth muscle actin (C6198; Sigma-Aldrich) or anti-collagen IV (ab19808; Abcam). Primary antibodies were visualized using Cy5- or Cy3-conjugated secondary antibodies (Jackson ImmunoResearch Laboratories). Vascular outgrowth, avascular area, and neovascular area were measured on flat-mounted retinas using Photoshop CS4 as previously described.²³ Vascular density at P4 was quantified on six fields/retina with each field representing 0.057 mm^2 located midway between the optic disk and the periphery and away from any main arteries or veins.

In Situ Hybridization

PGC-1 α probe was obtained by subcloning a 661-bp region of the mouse PGC-1 α cDNA (nucleotides 646 to 1307) into the pBluescript KS+ vector (Stratagene/Agilent Technologies, Santa Clara, CA) and transcribed *in vitro* to produce antisense and sense riboprobes labeled with digoxigenin. Flat-mounted retinas were hybridized and stained following the method previously described,²⁴ with some modifications. Samples were prehybridized at 65°C for 6 hours and hybridized at 60°C for 12 hours. The detection was performed with alkaline phosphatase-coupled anti-digoxigenin antibodies (11093274910, 1/2000; Roche Applied Science, Indianapolis, IN) overnight at 4°C . After washing, the chromogenic reaction was obtained with NBT/BCIP substrate (Promega, Madison, WI). After color development, the flat-mounted retinas were fixed in 4%

Table 1 List of Genes Studied

Symbol	Name
<i>ACTB</i>	Beta-actin
<i>TBP</i>	TATA box binding protein
<i>HPRT1</i>	Hypoxanthine phosphoribosyl-transferase 1
<i>B2M</i>	Beta-2-microglobulin
<i>COX5B</i>	Cytochrome c oxidase subunit Vb
<i>ATP5O</i>	ATP synthase, H^+ transporting, mitochondrial F1 complex, O subunit
<i>PPARGC1A</i> (alias PGC-1 α)	Peroxisome proliferator-activated receptor gamma, coactivator 1 alpha
<i>CYCS</i>	Cytochrome c, somatic
<i>ACADM</i> (alias MCAD)	Medium chain acyl CoA dehydrogenase
<i>VEGFA</i>	Vascular endothelial growth factor A
<i>PDGFB</i>	Platelet-derived growth factor beta polypeptide
<i>ANGPT1</i>	Angiopoietin 1
<i>ANGPT2</i>	Angiopoietin 2

Table 2 Primer Sequences Utilized for qPCR Analysis

Species	Symbol	Forward primer	Reverse primer
Mouse	<i>Actb</i>	5'-CCCTGTATGCCTCTGGTCGTACCAC-3'	5'-GCCAGCCAGGTCCAGACGCAGGATG-3'
Mouse	<i>Tbp</i>	5'-CCCTATCACTCCTGCCACACCAGC-3'	5'-GTGCAATGGTCTTTAGGTCAAGTTTACAGCC-3'
Mouse	<i>Hprt</i>	5'-GTTAAGCAGTACAGCCCCAAA-3'	5'-AGGGCATATCCAACAACAACTT-3'
Mouse	<i>B2m</i>	5'-GTGGCCCTTAGCTGTGCTCG-3'	5'-ACCTGAATGCTGGATAGCCTC-3'
Mouse	<i>Cox5b</i>	5'-GCTGCATCTGTGAAGAGGACAAC-3'	5'-CAGCTTGTAATGGGTTCCACAGT-3'
Mouse	<i>Atp5o</i>	5'-AGGCCCTTGCCAAGCTT-3'	5'-TTCTCCTTAGATGCAGCAGAGTACA-3'
Mouse	<i>PGC-1α*</i>	5'-GCTGCATGGTTCTGAGTGCTAAG-3'	5'-TCTGGTACCCAAGGCAGCC-3'
Mouse	<i>Cyts</i>	5'-GCAAGCATAAGACTGGACCAAA-3'	5'-TTGTTGGCATCTGTGTAAGAGAATC-3'
Mouse	<i>Acadm</i>	5'-CAGCTAGCCACTGACGCCGTGCAG-3'	5'-GCTCACGAGCTATGATCAGCCTCTG-3'
Mouse	<i>Vegfa</i>	5'-GAGGATGTCCTCACTCGGAT-3'	5'-TCTCAGACCACACTGAAGCC-3'
Mouse	<i>Pdgfb</i>	5'-CGAGCCAAGACGCCCTCAAGCTCGG-3'	5'-GGCCGCCTTGTCATGGGTGTGC-3'
Mouse	<i>Angpt1</i>	5'-GAAAATATGAAGTCGGAGATGGCCC-3'	5'-CCTATCTCAAGCATGGTGGCCGTGTG-3'
Mouse	<i>Angpt2</i>	5'-GCCACGGTCAACAACCTCGCTCC-3'	5'-GCAACCGAGCTCTTGAGTTGG-3'
Human	<i>HPRT1</i>	5'-TGGACAGGACTGAACGTCTTG-3'	5'-AGGGCATATCCAACAACAACTT-3'
Human	<i>ACTB</i>	5'-GAGCGCGGCTACAGCTT-3'	5'-TCCTTAATGTCACGCACGATTT-3'
Human	<i>COX5B</i>	5'-GGAAGACCCTAATTTAGTCCCCT-3'	5'-CCAGCTTGTAATGGGCTCCAC-3'
Human	<i>PGC-1α</i>	5'-GCTTTCTGGGTGGACTCAAGT-3'	5'-TCTAGTGTCTCTGTGAGGACTG-3'
Human	<i>VEGFA</i>	5'-CAACATCACCATGCAGATTATGC-3'	5'-CCCACAGGGATTTTCTTGCTTT-3'

*PPARGC1A is the official gene symbol for PGC-1α (*Pparg1α* in mouse)

paraformaldehyde, embedded in optimal cutting temperature compound, and cryosectioned.

Statistical Analysis

Values are expressed as mean ± SEM (unless specified otherwise), and statistical analysis was performed using an unpaired Student’s *t*-test.

Results

PGC-1α Is Strongly Expressed in Retinal Cells, and Is Dramatically Induced during Retinal Development

PGC-1α is a potent regulator of metabolism and angiogenesis in multiple tissues. The role of PGC-1α in the retina has not been investigated. To begin to investigate its role, the relative expression of PGC-1α in murine retinas was measured. Total RNA was prepared from various murine tissues, including retina, heart, and liver, using the Trizol method. The RNA was then reverse transcribed, and the expression of *PGC-1α* was measured by qPCR. As shown in [Figure 1A](#), PGC-1α is well expressed in the adult retina, at levels comparable to a number of tissues in which PGC-1α is well known to play important roles. This pattern of expression matches that observed in moderate-throughput microarray analyses publicly available, including from BioGPS, where expression of PGC-1α is strongly detected in a number of retinal components, including retinal pigment epithelium, iris, and ciliary body ([Supplemental Figure S1](#)).

Next, the expression of PGC-1α during postnatal development in the retina was measured. As shown in [Figure 1B](#), *PGC-1α* expression rises more than 20-fold during retinal development, beginning as early as P5 and peaking by P15

to P17. PGC-1α induction coincides with the rising expression of genes involved in mitochondrial function, well-known targets of PGC-1α (*CYCS*, *MCAD*; [Figure 1C](#)), as well as a number of angiogenic genes such as *VEGFA*, *PDGFB*, and *ANG2* ([Figure 1D](#)). Interestingly, although expression of proangiogenic factors reaches its peak at P7, the time of maximal vascular outgrowth, and then declines during the later stages of retinal development (P12 to P15) to allow for vascular plexus remodeling,²⁵ PGC-1α expression remains high, suggesting that sustained expression of PGC-1α may be required for retinal homeostasis beyond P12. We next used *in situ* hybridization to determine the PGC-1α expression pattern in the retina. At P7.5, PGC-1α expression is seen prominently in the ONL that contains the differentiating photoreceptors (PR), as well as more weakly in the INL and GCL ([Figure 1E](#)). In the adult retina, PGC-1α expression was more evenly distributed across all of the cellular layers ([Figure 1E](#)). PGC-1α is thus well expressed in the retina, and is strongly induced during early postnatal retinal development, coincident with physiological vascularization of the retina.

PGC-1α Regulates VEGFA Expression in Multiple Retinal Cell Types

The data above and our studies in skeletal muscle^{11,26} suggested that PGC-1α might regulate VEGFA and angiogenesis in the retina. To test this, a number of retinal cell lines were infected with adenovirus expressing PGC-1α, versus GFP control virus, and VEGFA expression was measured by qPCR 48 hours later. As shown in [Figure 2](#), A–D, delivery of PGC-1α by adenoviral infection efficiently induced the expression of *Cox5b*, a well-established mitochondrial target of PGC-1α, in a number of retinal cells, including Müller (glial) cells (MIO-M1) ([Figure 2D](#)), ganglion cells (RGC5) ([Figure 2A](#)),

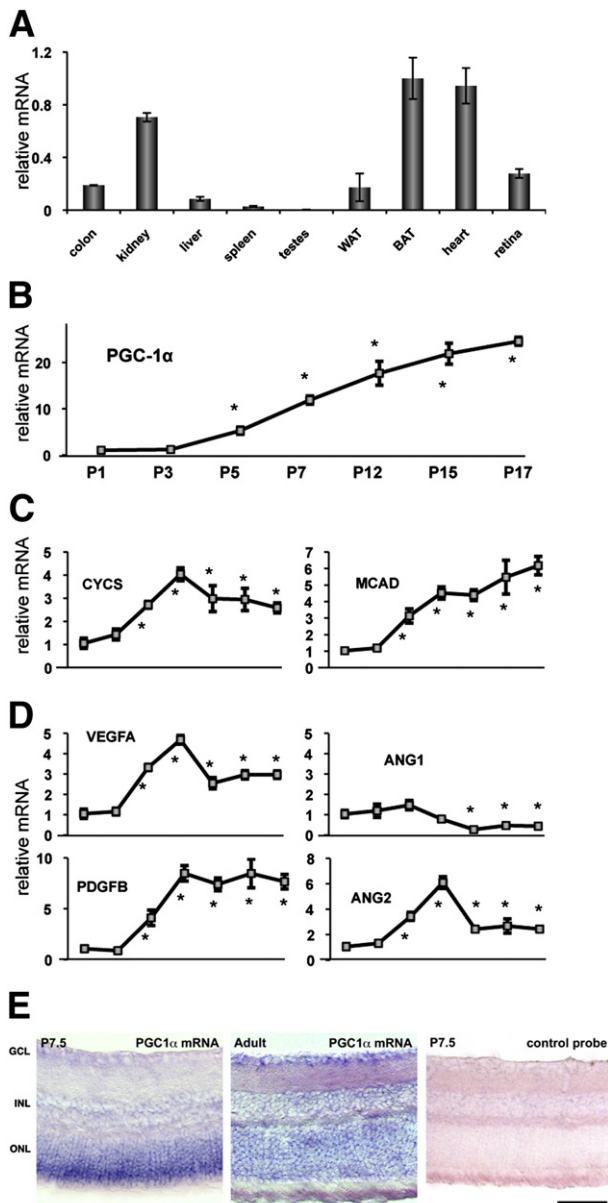


Figure 1 PGC-1 α expression in the retina and during retinal development. **A:** RNA from the indicated adult murine tissues was extracted and subjected to RT-qPCR for PGC-1 α . **B–D:** RNA from retinas of WT mice at age postnatal day 1 (P1) to P17 were harvested and subjected to RT-qPCR. The expression levels of PGC-1 α (**B**) and its downstream target genes, *CYCS* and *MCAD* (**C**), were increased with development with a surge from P3 to P7. The developmental expression curve of PGC-1 α also correlated with VEGFA, PDGFB, and ANG2 expression during the early stage of vascular outgrowth (up to P7). However, high PGC-1 α expression is maintained during the later stage of retinal development, whereas VEGFA expression is repressed (**D**). * $P < 0.05$ versus P1. **E:** *In situ* hybridization for PGC-1 α in P7.5 and adult retina. Scale bar = 50 μ m.

PR (661W) (Figure 2B), and retinal pigment epithelial cells (ARPE-19) (Figure 2C). Importantly, PGC-1 α also efficiently induced the expression of VEGFA in the same cells (Figure 2, A–D). Multiple retinal cell types, including astrocytes, ganglion cells, and RPE cells, have been shown to express VEGF under normal and pathological conditions.²⁷ However,

Müller cells are thought to be the main source of VEGFA in the inner retina in response to hypoxia.²⁸ We, therefore, focused our attention on this cell type. MIO-M1 cell lines stably expressing PGC-1 α , versus empty control, were generated by retroviral infection. PGC-1 α protein expression was increased approximately twofold (Figure 2E, inset). This moderate induction of PGC-1 α efficiently induced *Cox5b* (Figure 2E). The cells were then placed in low-serum medium, with and without hypoxia, to mimic as much as possible the ischemic environment of the retina. PGC-1 α overexpression significantly augmented the hypoxic induction of both VEGFA expression (Figure 2F) and secretion (Figure 2G) in these cells. Conversely, inhibition of PGC-1 α by small hairpin RNA (shPGC-1 α) in MIO-M1 cells significantly suppressed normal and hypoxia-induced VEGFA expression (Figure 2H). PGC-1 α thus regulates VEGFA expression in a number of retinal cell types, including Müller cells, in both normoxic and hypoxic conditions.

Vascular Development Is Abnormal in the Retinas of Mice Lacking PGC-1 α

The significant up-regulation of PGC-1 α expression during retinal postnatal development and its effect on VEGFA expression in various retinal cells suggest that PGC-1 α may play an important role during retinal vascular outgrowth. To test this, retinal flat mounts were obtained from P4 PGC-1 α -deficient mice, versus their littermate wild-type (WT) controls, and stained with the endothelial cell marker isolectin B4. PGC-1 α ^{−/−} mice have been previously described,¹⁷ but the effects of PGC-1 α deficiency on the retinal vasculature have not been reported. As shown in Figure 3, PGC-1 α ^{−/−} mice display a significant inhibition of the superficial vascular plexus outgrowth, as evidenced by a reduced vascular radius and area. This inhibition was associated with decreased number of tip cells at the vascular leading front and a moderate, but significant, reduction of capillary density (Figure 3).

VEGFA is also important for arterial specification of retinal vessels.²⁹ We therefore characterized the vascular remodeling of PGC-1 α ^{−/−} by co-staining P13.5 flat-mounted retinas with isolectin B4 and smooth-muscle actin, a marker for arterialized vessels (Figure 4A). At this stage, the retinal vascular network is matured into well-defined arterioles, venules, and capillaries. Arterioles and venules sprouting from the optic disk can be morphologically distinguished by their lumen size (larger in venules), the presence of a capillary-free zone around the arterioles, and the extent of smooth muscle cell coverage (stronger on arterioles). Although WT animals displayed an average of five main arteries and vein pairs sprouting from the optic disk, a significant reduction of the number of major vessels pairs was observed in 27% of the PGC-1 α ^{−/−} animals (Figure 4B). However, each pair maintained a proper arterial–venous specification. This phenotype was not associated with abnormal astrocyte network organization (not shown) or altered smooth muscle cell coverage. Interestingly,

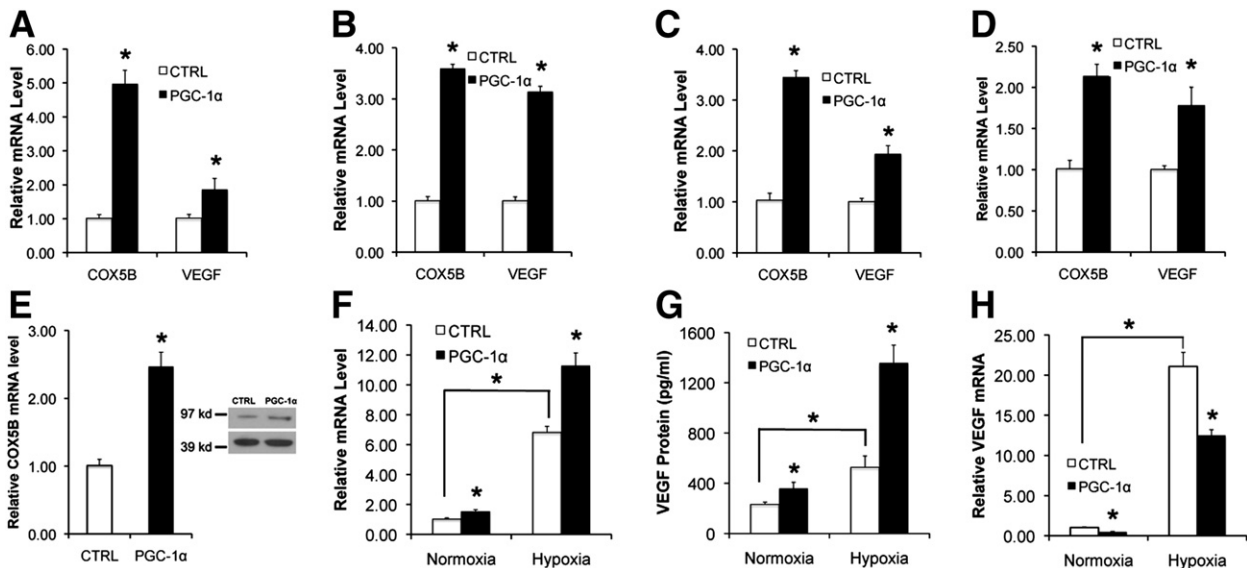


Figure 2 PGC-1 α regulates VEGFA in retinal cells. RGC5 (A), 661W (B), ARPE-19 (C), and MIO-M1 (D) were infected with adenovirus expressing mouse PGC-1 α or GFP (as negative control). Forty-eight hours postinfection, RNA was isolated and gene expression measured by qPCR. VEGFA was up-regulated two- to threefold in all cells. MIO-M1 were infected with retrovirus carrying vacant or mouse PGC-1 α plasmids. PGC-1 α expression at the protein level was elevated with induction of its target genes (E). PGC-1 α -dependent up-regulation (F) and secretion (G) of VEGF in MIO-M1 cells is enhanced by hypoxia. PGC-1 α knockdown by shRNA inhibits VEGFA expression in normoxic and hypoxic conditions (H). * $P < 0.05$.

the vascular density of the P13.5 PGC-1 α ^{-/-} retinas appeared normal, in contrast to P4.5 (Figure 3), suggesting that PGC-1 α deficiency delays vascular outgrowth, but does not reduce final vascular density or disrupt arterial–venous differentiation. Together, these results indicate that PGC-1 α contributes to normal vascularization of the developing retina.

Despite these vascular anomalies observed during early retinal development, the ocular structures and retinal layers appeared otherwise normal in adult PGC-1 α ^{-/-} mice, as seen by H&E-stained sections (Figure 5, A and B). SD-OCT imaging through the optic disk revealed also a normal retinal configuration (Figure 5C). Quantification of the ONL thickness confirmed the absence of obvious degenerative processes in adult PGC-1 α ^{-/-} mice (Figure 5D).

PGC-1 α ^{-/-} Mice Are Protected Against ROP in the OIR Model

ROP is marked by excess neovascularization in response to tissue ischemia. In light of the synergetic effect of PGC-1 α overexpression and hypoxia observed on VEGFA levels in MIO-M1 cells, we reasoned that PGC-1 α deficiency may blunt the excess neovascularization that occurs during ROP. To test this, the murine OIR model that recapitulates some of the key features of ROP was used. In this model, 7-day-old pups are placed with their mother in a hyperoxic chamber (75% O₂), where excess tissue oxygenation blunts the hypoxic drive for developmental angiogenesis. On day 12, the pups are returned to ambient air (21% O₂), where the now blunted vascular trees can no longer sustain tissue oxygenation. Retinal ischemia ensues, leading to disorganized angiogenesis and pathogenic neovascularization (Figure 6A).

We have shown previously that PGC-1 α expression is increased in skeletal muscle cells by ischemia-like conditions.¹¹ To test whether this is also the case in retinas subjected to OIR, we examined the expression of PGC-1 α in retinas isolated from P12 to P17 mice exposed to OIR. When measured in whole retinas, PGC-1 α expression appeared unchanged either by the hyperoxic treatment (P12, Figure 6B) or during the hypoxic phase of the model (P12 + 6 hours to P17, Figure 6B). By contrast, VEGFA was strongly down-regulated at P12 and then rapidly and significantly induced by the relatively hypoxic retina (Figure 6B). We hypothesized, however, that PGC-1 α may be regulated differently in different retinal layers. Laser-captured retinal layers followed by qPCR revealed that PGC1 α is expressed quite differently in the retinal layers. The strongest expression of PGC1 α is detected in the photoreceptor outer nuclear layer (ONL), followed by the INL, whereas the GCL expresses a much lower basal level of PGC-1 α (Figure 6D). The effects of OIR on PGC-1 α expression were remarkably layer specific. PGC1 α was strikingly induced in the INL (by over 190-fold), whereas it was reduced about 60% in the ONL, and slightly (but not significantly) induced in the GCL (Figure 6D). When integrated over the entire retina (Figure 6B), the strong expression of PGC-1 α in the ONL and its repression by OIR thus completely masked the dramatic induction of PGC-1 α in the INL (Figure 6D). The INL contains the Müller cells, the major source of VEGF during OIR.²⁸ These data thus indicate that PGC-1 α is likely potentially induced in Müller cells by the relative ischemia induced by the OIR model.

The data above also strongly suggest that PGC-1 α up-regulation could be involved in the pathological induction of

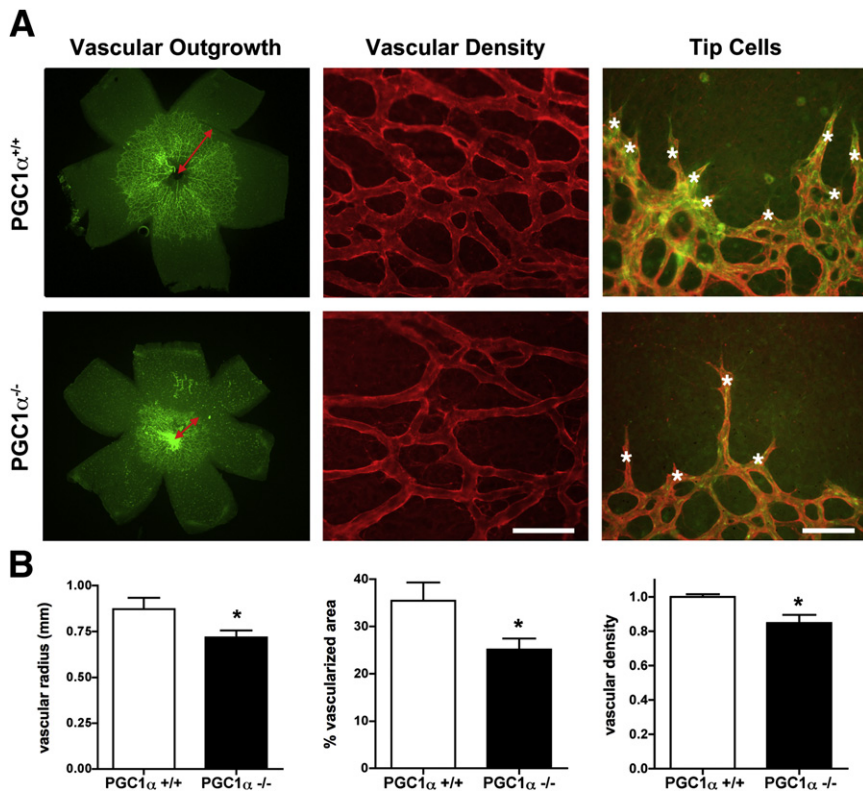


Figure 3 Delayed retinal vascular development and decreased capillary density in *PGC-1 α ^{-/-}* mice. Developmental retinal vessels outgrowth was evaluated at P4 on isolectin-B4 (green) and/or collagen IV (red) stained flat-mounts (**A**) and quantified (**B**). *PGC-1 α ^{-/-}* pups showed reduced vascular radius (red arrows) and area compared to WT littermates (**A** and **B**). High-magnification micrographs of the vascular front revealed a decreased number of tip cells (asterisks) in *PGC-1 α ^{-/-}* compared to WT (**A**). Vascular density was quantified on collagen IV-stained P4 retina flat-mounts and revealed a significant decrease of capillary density in *PGC-1 α ^{-/-}* mice ($n = 5$ to 7). * $P < 0.05$.

VEGFA and vessel proliferation during the OIR model of ROP. Therefore, we next analyzed the effect of PGC1 α deficiency in the OIR model. As shown in Figure 7A, and quantified in Figure 7B, pathological neovascularization covers approximately 11% of the area of flat mounts of WT P17 mice that have undergone OIR. By contrast, only about 7% of the area of retinas from OIR *PGC-1 α ^{-/-}* mice have

signs of pathological angiogenesis ($P < 0.01$), a reduction of about 36%. Inhibition of PGC-1 α is thus protective in the OIR model of ROP.

Pathological angiogenesis in the OIR model is triggered by hypoxia, which is proportional to the avascular area created by the hyperoxic treatment. To test whether reduced angiogenesis in the *PGC-1 α ^{-/-}* OIR mice reflects a decreased area at risk after the hyperoxic treatment, a separate cohort of mice was sacrificed at P12, the end of the hyperoxic treatment. As shown in Figure 7, C and D, the avascular area at P12 was similar between *PGC-1 α ^{+/+}* and *PGC-1 α ^{-/-}* animals. The reduced pathological angiogenesis observed in *PGC-1 α ^{-/-}* mice in the OIR model (Figure 7, A and B) thus does not reflect differences in avascular area at the end of the hyperoxic treatment, and instead, most likely reflects decreased expression of VEGFA in response to the relative tissue ischemia after withdrawal from hyperoxia. To test this, total RNA was prepared from P17 retinas of *PGC-1 α ^{-/-}* and WT mice that had undergone the OIR model. As shown in Figure 7E, the expression of VEGFA was significantly reduced in *PGC-1 α ^{-/-}* retinas. Together, these data show that deletion of PGC-1 α protects against pathological neovascularization in the OIR model, likely via reduced expression of VEGFA.

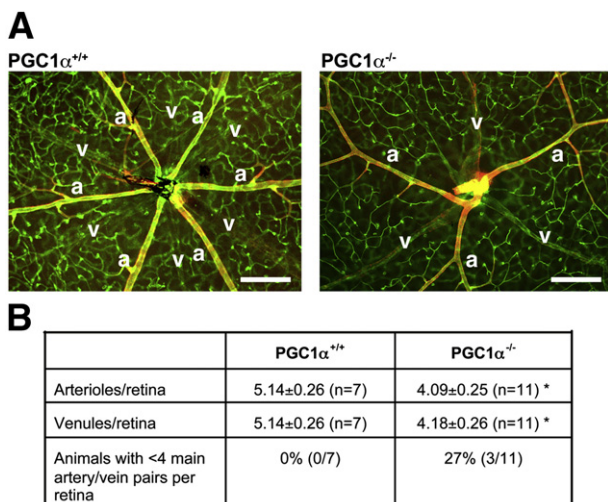


Figure 4 Reduced number of main arteries and veins in *PGC-1 α ^{-/-}* mice. **A**: Flat-mounted retinas of WT and PGC-1 α knockout littermates at P13.5 were costained with isolectin B4 (green) and smooth-muscle actin (red) to differentiate veins (v) and arteries (a). The number of main arteries and veins was reduced in *PGC-1 α ^{-/-}* (**B**) (mean \pm SD, $n = 7$ to 11) * $P < 0.05$.

Discussion

We show here that PGC-1 α regulates normal and pathological angiogenesis in the retina. Absence of PGC-1 α in knockout mice leads to defects in normal vascular

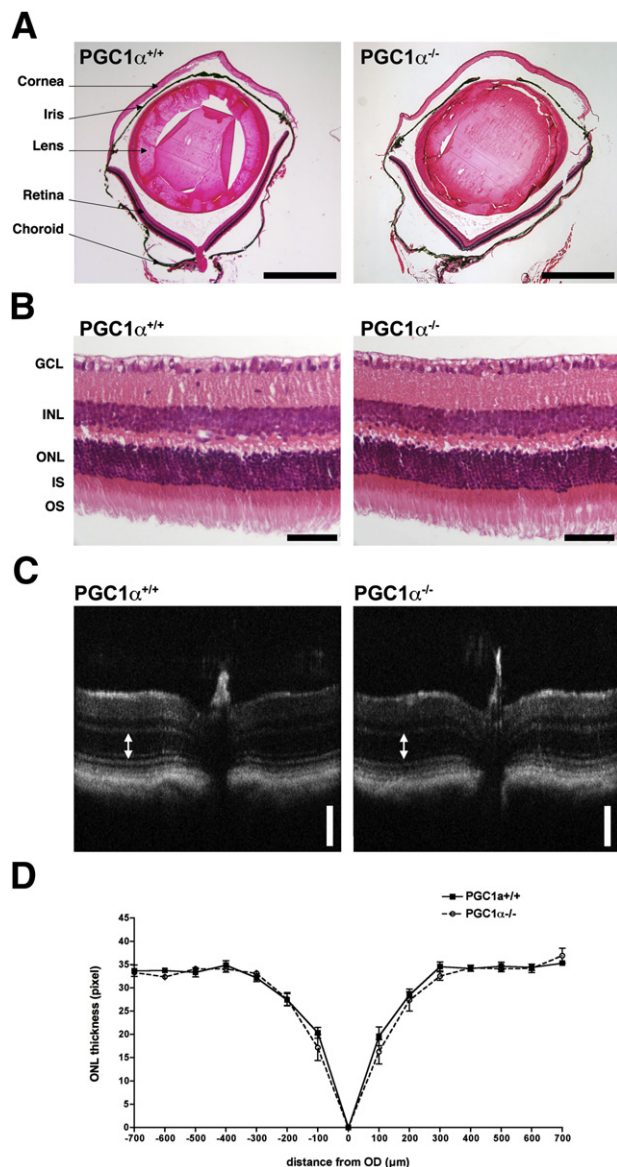


Figure 5 Normal ocular and retinal structures in *PGC-1α*^{-/-} mice. **A** and **B**: H&E-stained sagittal ocular sections from 8-week-old *PGC-1α*^{+/+} (WT) and *PGC-1α*^{-/-} mice. **A**: Low magnification showing normal ocular structures; scale bars = 500 μm. **B**: Higher magnification showing no abnormal retinal organization or layers thickness in *PGC-1α*^{-/-} mice; scale bars = 50 μm. **C**: Representative pictograms of SD-OCT recordings from WT and *PGC-1α*^{-/-} mice, the ONL is indicated by **double-headed arrows**. Scale bars = 100 μm. **D**: ONL thickness from OCT recordings were quantified every 100 μm from the optic nerve head (OD) (mean ± SD, *n* = 3 to 6). GCL, ganglion cell layer; INL, inner nuclear layer; IS, inner segment; ONL, outer nuclear layer; OS, outer segment.

outgrowth, while at the same time diminishing excessive pathological angiogenesis in the OIR model.

We show that *PGC-1α* regulates VEGFA in a number of retinal cell types *in vitro*. It is likely that the predominant effect of *PGC-1α* on retinal neovascularization is mediated in Müller cells, which are thought to be the main source of VEGFA³⁰ and a major contributor to hypoxia-induced

vascular leakage and neovascularization.³¹ Consistent with this, hypoxic conditions enhanced *PGC-1α*-dependent VEGFA up-regulation in Müller cells (Figure 2). Other cells could of course also be at play. Retinal neovascularization is regulated by complex interactions between vascular, glial, and neuronal cells.³² *PGC-1α* is highly expressed in

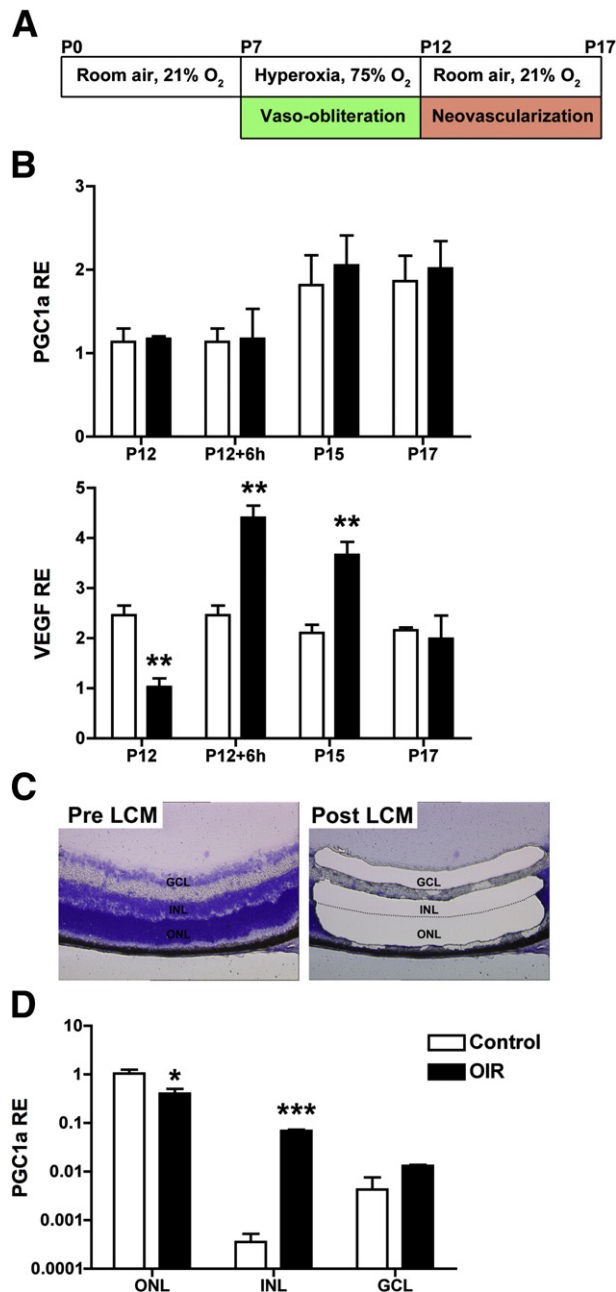


Figure 6 Region-specific regulation of *PGC-1α* expression during OIR. **A**: Schematic representation of the OIR model. **B**: qPCR quantification of *PGC-1α* and VEGFA mRNA in total retinas from P12 to P17 in control (white bars) and OIR (black bars) WT mice. **C**: Representative pictures of retinal sections before (Pre LCM) and after (Post LCM) laser capture microdissection. **D**: mRNA quantification by qPCR from laser-captured ONL, INL, and GCL of P17 control and OIR retinas (log y axis). Results are expressed as RE (relative expression) normalized to housekeeping genes (mean ± SEM, *n* = 3 to 4). **P* < 0.05, ***P* < 0.01, and ****P* < 0.001.

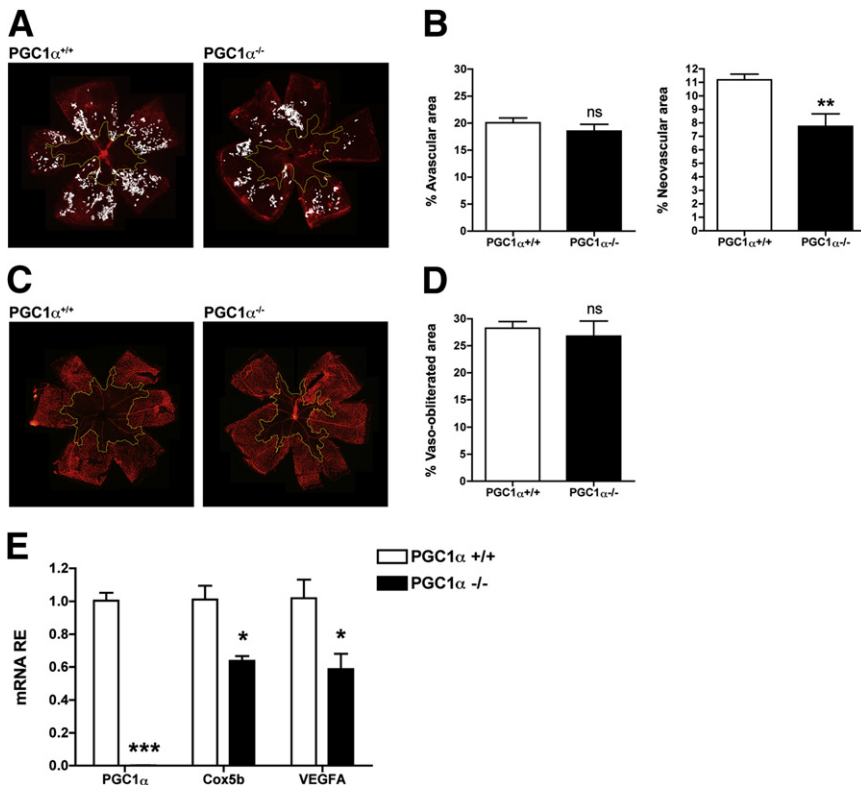


Figure 7 *PGC-1 α ^{-/-}* mice are protected against OIR. Oxygen-induced retinopathy (OIR) was induced by exposing *PGC-1 α ^{+/+}* (WT) and *PGC-1 α ^{-/-}* mouse pups to 75% oxygen from P7 to P12. **A** and **B**: At P17, retinas were harvested and stained with isolectin-B4. The vaso-obliterated areas (yellow outline) and neovascular areas (marked in white) were quantified using Photoshop CS4 software. Loss of *PGC-1 α* did not affect the avascular zone but significantly reduced the neovascular area ($n = 7$ to 9). $^{**}P < 0.01$. **C** and **D**: Representative pictograms (**C**) and quantification (**D**) of the central vaso-obliteration induced by hyperoxia at P12 ($n = 7$ to 12). ns, no statistical difference. **E**: qPCR analysis of total retina mRNA isolated from P17 animals exposed to OIR model revealed a significant reduction in *Cox5b* and *VEGFA* expression in *PGC-1 α ^{-/-}* mice compared to *PGC-1 α ^{+/+}* ($n = 4$). $^{*}P < 0.05$, $^{***}P < 0.001$.

developing PR (Figure 1) and was recently shown to be involved in PR susceptibility to light damage.¹⁶ Even though the PR do not appear to be a major source of proangiogenic molecules even under severe hypoxia, the hypoxic state of the PR can affect *VEGFA* expression and the subsequent angiogenic response.³³ However, since *PGC-1 α* deficiency does not cause retinal degeneration (Figure 5 and Egger et al¹⁶), it seems unlikely that *PGC-1 α* -dependent modulation of PR metabolism drives the reduced oxygen-dependent neovascularization that we observed. *PGC-1 α* could also be involved in the homeostasis of endothelial cells.³⁴ However, *PGC-1 α* expression in endothelial cells is extremely low when compared to other cell types and, in particular, to Müller cells (Supplemental Figure S2), suggesting that the role of *PGC-1 α* is likely much greater in Müller cells. Finally, it is formally possible that some aspect of the phenotype observed here reflects alterations in systemic metabolism in the *PGC-1 α ^{-/-}* mice. The simplest interpretation of our findings, however, is that the predominant effect of *PGC-1 α* is mediated in Müller cells, which are thought to be the strongest secretors of *VEGFA*.³⁰ Precise characterization of function of *PGC-1 α* in each cell type will require cell-specific deletion with available floxed alleles of *PGC-1 α* .

Angiogenesis in the retina, in particular in response to physiological and pathological hypoxia has been thought to be mediated primarily by the HIF-1 pathway, even though evidence suggests that other pathways must exist.¹⁰ We have shown previously that the induction of *VEGFA* and angiogenic factors by *PGC-1 α* in skeletal muscle is

independent of HIF-1 α , occurring instead by coactivation of the orphan nuclear receptor estrogen-related receptor α (*ERR α*).¹¹ The data presented here demonstrate that this pathway is also likely at play in the retina. Interestingly, we did not observe in *PGC-1 α* -deficient mice any changes in the extent of oxygen-induced vaso-obliteration in the OIR model, suggesting that, contrary to what occurs with HIF-1 proteins,³⁵ *PGC-1 α* is not involved in the maintenance of the trophic factors that prevent microvascular obliteration. It will be of interest to study retinal development and response to OIR in *ERR α ^{-/-}* mice. It will also ultimately be of interest to attempt to intervene pharmacologically in this novel pathway. Screens to identify small molecules that modulate *PGC-1 α* have yielded some results, for example, but remain in the early stages.³⁶

Some aspects of the phenotypes we observed in unchallenged *PGC-1 α ^{-/-}* mice were incompletely penetrant (eg, Figure 4). This may reflect effects of variable genetic modifiers and/or variable compensation by other pathways. *PGC-1 β* , for example, regulates many of the same pathways as *PGC-1 α* , including angiogenesis in skeletal muscle.³⁷ We did not observe compensatory up-regulation of *PGC-1 β* mRNA in *PGC-1 α ^{-/-}* mice, but compensation may have occurred at the posttranscriptional level. It will be of interest, therefore, to evaluate deletion of both *PGC-1 α* and β simultaneously. This will require conditional deletion in the appropriate cell type, since *PGC-1 α/β* doubly deleted mice die at birth.³⁸

The *PGC-1 α* -regulated pathway in the eye likely provides an important node for regulation by multiple

physiological cues. Hypoxia is not the only challenge that ischemic tissues face. Insufficient blood flow also leads to deprivation of nutrients, pH changes, dramatic changes in intermediate metabolism and cellular redox state, and accumulation of numerous extracellular molecules. The role that these metabolic events play in regulating angiogenesis is not well understood. For example, Sapieha et al³⁹ recently showed that the hypoxic retina accumulates extracellular succinate, which directly stimulates ganglion cells to secrete VEGFA and other angiogenic factors independently from the HIF pathway. Thus, the complex metabolic events that occur during ischemia are clearly linked to the angiogenic response, but the mechanisms involved remain incompletely resolved. PGC-1 α is extensively regulated, both at the transcriptional and posttranslational levels, by upstream signaling cascades including cAMP, mitogen-activated protein kinase, and powerful metabolic sensors such as AMP-activated protein kinase and sirtuin.¹⁴ PGC-1 α thus integrates multiple metabolic signals in addition to hypoxia, and is in an ideal position to link those signals to angiogenesis in the eye.

In summary, we show here that PGC-1 α regulates VEGFA and angiogenesis in the retina under both physiological and pathophysiological conditions. Further study of this novel pathway may lead to new insight and approaches to treating a variety of retinal pathologies marked by inappropriate and deranged neovascularization, including ROP, but also “wet” aged-related macular degeneration and diabetic retinopathy.

Acknowledgments

We thank Drs. Andrea Giani and Aristomenis Thanos (Massachusetts Eye and Ear Infirmary, Boston) for their assistance in SD-OCT image acquisition.

Supplemental Data

Supplemental material for this article can be found at <http://dx.doi.org/10.1016/j.ajpath.2012.09.003>.

References

1. Yu DY, Cringle SJ: Oxygen distribution and consumption within the retina in vascularised and avascular retinas and in animal models of retinal disease. *Prog Retin Eye Res* 2001, 20:175–208
2. Saint-Geniez M, D'Amore PA: Development and pathology of the hyaloid, choroidal and retinal vasculature. *Int J Dev Biol* 2004, 48:1045–1058
3. Engerman RL, Pfaffenbach D, Davis MD: Cell turnover of capillaries. *Lab Invest* 1967, 17:738–743
4. Phelps DL: Retinopathy of prematurity: an estimate of vision loss in the United States—1979. *Pediatrics* 1981, 67:924–925
5. Sapieha P, Joyal JS, Rivera JC, Kermorvant-Duchemin E, Sennlaub F, Hardy P, Lachapelle P, Chemtob S: Retinopathy of prematurity: understanding ischemic retinal vasculopathies at an extreme of life. *J Clin Invest* 2012, 120:3022–3032
6. Alon T, Hemo I, Itin A, Pe'er J, Stone J, Keshet S: Vascular endothelial growth factor acts as a survival factor for newly formed retinal vessels and has implications for retinopathy of prematurity. *Nat Med* 1995, 1:1024–1028
7. Chen J, Stahl A, Hellstrom A, Smith LE: Current update on retinopathy of prematurity: screening and treatment. *Curr Opin Pediatr* 2011, 23:173–178
8. Mintz-Hittner HA, Kennedy KA, Chuang AZ, BEAT-ROP Cooperative Group: Efficacy of intravitreal bevacizumab for stage 3+ retinopathy of prematurity. *N Engl J Med* 2011, 364:603–615
9. Arjamaa O, Nikinmaa M: Oxygen-dependent diseases in the retina: role of hypoxia-inducible factors. *Exp Eye Res* 2006, 83:473–483
10. Vinore SA, Xiao WH, Aslam S, Shen J, Oshima Y, Nambu H, Liu H, Carmeliet P, Campochiaro PA: Implication of the hypoxia response element of the Vegf promoter in mouse models of retinal and choroidal neovascularization, but not retinal vascular development. *J Cell Physiol* 2006, 206:749–758
11. Arany Z, Foo SY, Ma Y, Ruas JL, Bommi-Reddy A, Girnun G, Cooper M, Laznik D, Chinsomboon J, Rangwala SM, Baek KH, Rosenzweig A, Spiegelman BM: HIF-independent regulation of VEGF and angiogenesis by the transcriptional coactivator PGC-1 α . *Nature* 2008, 451:1008–1012
12. Kelly DP, Scarpulla RC: Transcriptional regulatory circuits controlling mitochondrial biogenesis and function. *Genes Dev* 2004, 18:357–368
13. Lin J, Handschin C, Spiegelman BM: Metabolic control through the PGC-1 family of transcription coactivators. *Cell Metab* 2005, 1:361–370
14. Handschin C, Spiegelman BM: Peroxisome proliferator-activated receptor gamma coactivator 1 coactivators, energy homeostasis, and metabolism. *Endocr Rev* 2006, 27:728–735
15. Arany Z: PGC-1 coactivators and skeletal muscle adaptations in health and disease. *Curr Opin Genet Dev* 2008, 18:426–434
16. Egger A, Samardzija M, Sothilingam V, Tanimoto N, Lange C, Salatino S, Fang L, Garcia-Garrido M, Beck S, Okoniewski MJ, Neutzner A, Seeliger MW, Grimm C, Handschin C: PGC-1 α determines light damage susceptibility of the murine retina. *PLoS One* 2012, 7:e31272
17. Lin J, Wu PH, Tarr PT, Lindenberg KS, St-Pierre J, Zhang CY, Mootha VK, Jager S, Vianna CR, Reznick RM, Cui L, Manieri M, Donovan MX, Wu Z, Cooper MP, Fan MC, Rohas LM, Zavacki AM, Cinti S, Shulman GI, Lowell BB, Krainc D, Spiegelman BM: Defects in adaptive energy metabolism with CNS-linked hyperactivity in PGC-1 α null mice. *Cell* 2004, 119:121–135
18. Smith LE, Wesolowski E, McLellan A, Kostyk SK, D'Amato R, Sullivan R, D'Amore PA: Oxygen-induced retinopathy in the mouse. *Invest Ophthalmol Vis Sci* 1994, 35:101–111
19. Vega RB, Huss JM, Kelly DP: The coactivator PGC-1 cooperates with peroxisome proliferator-activated receptor alpha in transcriptional control of nuclear genes encoding mitochondrial fatty acid oxidation enzymes. *Mol Cell Biol* 2000, 20:1868–1876
20. Puigserver P, Wu Z, Park CW, Graves R, Wright M, Spiegelman BM: A cold-inducible coactivator of nuclear receptors linked to adaptive thermogenesis. *Cell* 1998, 92:829–839
21. Vandesompele J, De Preter K, Pattyn F, Poppe B, Van Roy N, De Paep A, Speleman F: Accurate normalization of real-time quantitative RT-PCR data by geometric averaging of multiple internal control genes. *Genome Biol* 2002, 3:RESEARCH0034
22. Saint-Geniez M, Maharaj AS, Walshe TE, Tucker BA, Sekiyama E, Kurihara T, Darland DC, Young MJ, D'Amore PA: Endogenous VEGF is required for visual function: evidence for a survival role on Müller cells and photoreceptors. *PLoS ONE* 2008, 3:e3554
23. Connor KM, Krah NM, Dennison RJ, Aderman CM, Chen J, Guerin KI, Sapieha P, Stahl A, Willett KL, Smith LE: Quantification of oxygen-induced retinopathy in the mouse: a model of vessel loss, vessel regrowth and pathological angiogenesis. *Nat Protoc* 2009, 4:1565–1573

24. Saint-Geniez M, Argence CB, Knibiehler B, Audigier Y: The *mstr/apj* gene encoding the apelin receptor is an early and specific marker of the venous phenotype in the retinal vasculature. *Gene Expr Patterns* 2003, 3:467–472
25. Fruttiger M: Development of the retinal vasculature. *Angiogenesis* 2007, 10:77–88
26. Chinsomboon J, Ruas J, Gupta RK, Thom R, Shoag J, Rowe GC, Sawada N, Raghuram S, Arany Z: The transcriptional coactivator PGC-1 α mediates exercise-induced angiogenesis in skeletal muscle. *Proc Natl Acad Sci U S A* 2009, 106:21401–21406
27. Gariano RF, Gardner TW: Retinal angiogenesis in development and disease. *Nature* 2005, 438:960–966
28. Pierce EA, Avery RL, Foley ED, Aiello LP, Smith LE: Vascular endothelial growth factor/vascular permeability factor expression in a mouse model of retinal neovascularization. *Proc Natl Acad Sci U S A* 1995, 92:905–909
29. Stalmans I, Ng YS, Rohan R, Fruttiger M, Bouche A, Yuce A, Fujisawa H, Hermans B, Shani M, Jansen S, Hicklin D, Anderson DJ, Gardiner T, Hammes HP, Moons L, Dewerchin M, Collen D, Carmeliet P, D'Amore PA: Arteriolar and venular patterning in retinas of mice selectively expressing VEGF isoforms. *J Clin Invest* 2002, 109:327–336
30. Stone J, Itin A, Alon T, Pe'er J, Gnessin H, Chan-Ling T, Keshet E: Development of retinal vasculature is mediated by hypoxia-induced vascular endothelial growth factor (VEGF) expression by neuroglia. *J Neurosci* 1995, 15:4738–4747
31. Bai Y, Ma JX, Guo J, Wang J, Zhu M, Chen Y, Le YZ: Muller cell-derived VEGF is a significant contributor to retinal neovascularization. *J Pathol* 2009, 219:446–454
32. Vessey KA, Wilkinson-Berka JL, Fletcher EL: Characterization of retinal function and glial cell response in a mouse model of oxygen-induced retinopathy. *J Comp Neurol* 2011, 519:506–527
33. Lahdenranta J, Pasqualini R, Schlingemann RO, Hagedorn M, Stallcup WB, Bucana CD, Sidman RL, Arap W: An anti-angiogenic state in mice and humans with retinal photoreceptor cell degeneration. *Proc Natl Acad Sci U S A* 2001, 98:10368–10373
34. Valle I, Alvarez-Barrientos A, Arza E, Lamas S, Monsalve M: PGC-1 α regulates the mitochondrial antioxidant defense system in vascular endothelial cells. *Cardiovasc Res* 2005, 66:562–573
35. Duan LJ, Takeda K, Fong GH: Prolyl hydroxylase domain protein 2 (PHD2) mediates oxygen-induced retinopathy in neonatal mice. *Am J Pathol* 2011, 178:1881–1890
36. Arany Z, Wagner BK, Ma Y, Chinsomboon J, Laznik D, Spiegelman BM: Gene expression-based screening identifies microtubule inhibitors as inducers of PGC-1 α and oxidative phosphorylation. *Proc Natl Acad Sci U S A* 2008, 105:4721–4726
37. Rowe GC, Jang C, Patten IS, Arany Z: PGC-1 β regulates angiogenesis in skeletal muscle. *Am J Physiol Endocrinol Metab* 2011, 301:E155–E163
38. Lai L, Leone TC, Zechner C, Schaeffer PJ, Kelly SM, Flanagan DP, Medeiros DM, Kovacs A, Kelly DP: Transcriptional coactivators PGC-1 α and PGC-1 β control overlapping programs required for perinatal maturation of the heart. *Genes Dev* 2008, 22:1948–1961
39. Sapieha P, Sirinyan M, Hamel D, Zaniolo K, Joyal JS, Cho JH, Honore JC, Kermorvant-Duchemin E, Varma DR, Tremblay S, Leduc M, Rihakova L, Hardy P, Klein WH, Mu X, Mamer O, Lachapelle P, Di Polo A, Beausejour C, Andelfinger G, Mitchell G, Sennlaub F, Chemtob S: The succinate receptor GPR91 in neurons has a major role in retinal angiogenesis. *Nat Med* 2008, 14:1067–1076